A Solid Oxide Fuel Cell model to investigate load following and stability issues in distribution networks

S. Massucco, *IEEE M.*, A. Morini, *IEEE M.*, *G.* Petretto, A. Pitto, *IEEE St. M.*, F. Silvestro, *IEEE M.*

***Abstract*— The increase of DG penetration in the distribution networks makes more and more interesting the investigation of security issues which are typical of the large transmission grids (transient stability, voltage stability and small signal stability) as well as the study of the DG responses to load changes in the grid.**

This paper presents the model of a Solid Oxide Fuel Cell (SOFC) dedicated to perform dynamic simulations on MV distribution networks. In particular in the present paper transient stability and load following issues are tackled.

The first part of the paper is aimed at describing the model of the SOFC which is then used in the test system. As also a gas turbine is inserted into the test system, a brief look at the gas turbine model is mandatory. The aforementioned models include both the slow dynamics (GT prime mover, electrochemical system time constants for SOFC) necessary to study the DG response to load variations and the fast dynamics (e.g the power converter control and protection systems for SOFCs) necessary to study the transient stability related issues. The results of the analysis (carried out on a test MV distribution network) are reported and some conclusions are drawn.

***Index Terms*— Distributed Generation, Transient Stability, Load Following, Solide Oxide Fuel Cell, Gas Turbine**

I. Introduction

Nowadays, Distributed Generation (DG) is emerging as a complementary infrastructure to the traditional central power plants.

The major drives to this direction derive from the growing difficulty to identify adequate sites for large power plants and from the greenhouse gases threaten, which induced industrialized countries to commit themselves to reducing carbon dioxide emissions.

The deployment of Distributed Resources (DR) on distribution networks could potentially increase their reliability and lower the cost of power delivery by placing energy sources nearer to the demand centres. By providing a way to by-pass conventional power delivery systems, DR could also offer additional supply flexibility [1].

Among the different technologies available for DG, fuel cells are able to cover a large range of ratings and are very appealing because they have high efficiencies also on medium-small ratings and/or at partial loads, use hydrogen as fuel and have almost zero impact on environment. Moreover they have no rotating parts, thus they need little maintenance and they are highly reliable.

The term "fuel cell" includes different technologies which differ for the type of electrolyte: Molten Carbonate Fuel Cell (MCFC), AFC (Alkaline Fuel Cell), PAFC (Phosforic Acid Fuel Cell), PEFC (Polymer Electrolyte Fuel Cell) and SOFC (Solid Oxide Fuel Cell). They have different features (different operating temperatures, power densities and efficiencies) [2].

This paper is aimed at presenting a model for the SOFC. The model includes the dynamics of the partial pressures of reactants and products, the control of the utilization factor and the controls of the converters. The model is validated on a test system by studying its response to load changes and the impact on the transient stability of the grid. Section II is devoted to describe the SOFC model. Section III presents a brief introduction to the GT model adopted for the simulations. In Section IV the test system is described, while in Section V and Section VI the load following and the transient stability studies are performed using time domain simulations. In Section VII some conclusions are drawn.

II. The Proposed Model of SOFC

A. Overview

The fuel cells considered in the present paper are SOFCs. These devices represent the fuel cell with the longest continuous development period, starting in the late 1950s, several years before the AFC [2]. Because the electrolyte is solid, the cell can be cast into various shapes, such as tubular, planar, or monolithic. The solid ceramic construction of the unit cell alleviates any corrosion problems in the cell. The solid electrolyte also allows precise engineering of the three-phase boundary and avoids electrolyte movement or flooding in the electrodes. The kinetics of the cell are relatively fast, and CO is a directly useable fuel as it is in the MCFC. There is no need for CO_2 at the cathode as with the MCFC. The materials used in SOFC are modest in cost. Thin-electrolyte planar SOFC unit cells have been demonstrated to be capable of power densities close to those achieved with PEFC. As with

S. Massucco, A. Morini, A. Pitto, F. Silvestro are with UGDIE – Electrical Engineering Department, University of Genova, Italy. Email: massucco@die.unige.it, amorini@epsl.die.unige.it, apitto@die.unige.it, fsilvestro@die.unige.it.
G. Petretto is with ENEL RICERCA, Pisa, Italy. Email: giacomo.petretto@enel.it.

978-1-4244-2235-7/09/$25.00 ©2009 IEEE

the MCFC, the high operating temperature allows to use most of the waste heat for cogeneration or in bottoming cycles. Efficiencies ranging from around 40 percent (simple cycle small systems) to over 50 percent (hybrid systems) have been demonstrated.

However, the high temperature of the SOFC has its drawbacks. There are thermal expansion mismatches among materials, and sealing between cells is difficult in the flat plate configurations. The high operating temperature places severe constraints on materials selection and results in difficult fabrication processes. Corrosion of metal stack components (such as the interconnects in some designs) is a challenge. These factors limit stack-level power density (though significantly higher than in PAFC and MCFC), and thermal cycling and stack life (though the latter is better than for MCFC and PEFC).

The SOFC model includes the following subsystems:

- The electrochemical system which is characterized by relatively slow time constants
- The power conditioning unit which has a fast response

In SOFC the chemical reactions are [2]:

at the anode

$$H_2 + O^{=} \rightarrow H_2O + 2e^{-}$$

at the catode

$$\tfrac{1}{2} O_2 + 2e^{-} \rightarrow O^{=}$$

On the basis of the electrochemical relationships, the molar flow of hydrogen is linked to the cell current through the formula:

$$q^r_{H_2} = \frac{N_0 I}{2F} = 2K_r I \qquad (1)$$

where I is the cell current (in A), N_0 the number of cells of SOFC, F is the Faraday constant (equal to 96485 C/mol) and $q^r_{H_2}$ is the molar flow of hydrogen (in mol/s).

B. *The electrochemical subsystem*

The electrochemical system modeling is carried out under the following assumptions [3]:

- Gases are ideal.
- The channels which transport the gases along the electrodes have fixed volume, but their length is small so that it is necessary to define only one pressure value in their interior.
- The cell temperature is stable all the time.
- The only loss source is the ohmic loss because the operating conditions are not close to the inferior and superior limits of current
- Nerst equation can be applied

Taking into account the ideal gas law, the flow balance of each reacting gas and (1), three dynamic equations can be deduced to describe the electrochemical model of the cell:

$$p_{H_2} = \frac{1/K_{H_2}}{1 + s\tau_{H_2}} \left(q^{in}_{H_2} - 2K_r I \right) \qquad (2)$$

$$p_{H_2O} = \frac{1/K_{H_2O}}{1 + s\tau_{H_2O}} \left(2K_r I \right) \qquad (3)$$

$$p_{O_2} = \frac{1/K_{O_2}}{1 + s\tau_{O_2}} \left(q^{in}_{O_2} - K_r I \right) \qquad (4)$$

The SOFC model, [3]-[4], has been implemented in DigSILENT PowerFactory [5]. Fig. 1 shows the model of the electrochemical subsystem.

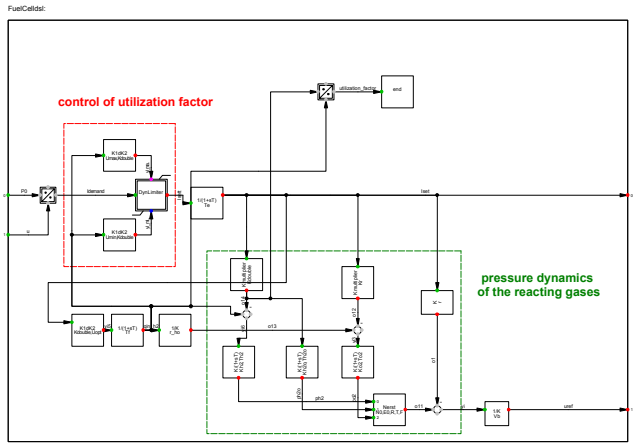

Fig. 1. The model of the electrochemical subsystem of SOFC

The model includes a limiter on the utilization factor U which is defined as the ratio between the reacted hydrogen molar flow and the overall inlet H_2 molar flow ($U = q^r_{H_2} / q^{in}_{H_2}$).

This discrete control limits the fuel utilization within an admissible range (typically 0.8-0.9). In fact if the fuel utilization drops below a certain limit, the cell voltage will rise rapidly. If the fuel utilization increases beyond a certain value, the cells may suffer from fuel starvation and be permanently damaged.

C. *Power electronics control and protection*

As for the power conditioning unit, as the fuel cell produces a DC current, it is necessary to interface the cell to the AC grid by adequate power converters. In particular, the power conditioning is composed by two converters:

1. a DC/DC booster used to raise the cell voltage level (which is usually too low to properly feed the inverter)
2. a Voltage Source Inverter for the cell interface to the grid

Literature proposes different control strategies for fuel cells [2][6]. The control strategy adopted in this paper acts as follows: the voltage at the DC link is controlled by the DC/DC converter, while the inverter is characterized by a typical PQ controller based on Park's transformations.

For transient stability issues it is also important to model the protection scheme of the fuel cell. In fact the fuel cells, as well

as all the other DG sources which are interfaced to the grid by power converters, need protection schemes able to protect power electronics devices. In particular in the present paper an undervoltage protection (type 27) is modeled: it disconnects the fuel cell plants from the grid when a minimum voltage threshold is reached (typically 80%).

III. A BRIEF LOOK AT THE GAS TURBINE MODEL

Gas turbines [7] are frequently used for CHP (Combined Heat and Power) applications and represent a promising DG source also because of the need of little maintenance with respect to internal combustion engines.

The gas turbine model, adapted from [8] [9], is composed by the following subsystems:

- A thermo-mechanical subsystem which simulates the prime mover
- A subtransient model of a synchronous generator

Fig. 2 shows the thermo-mechanical subsystem modeled for the present studies.

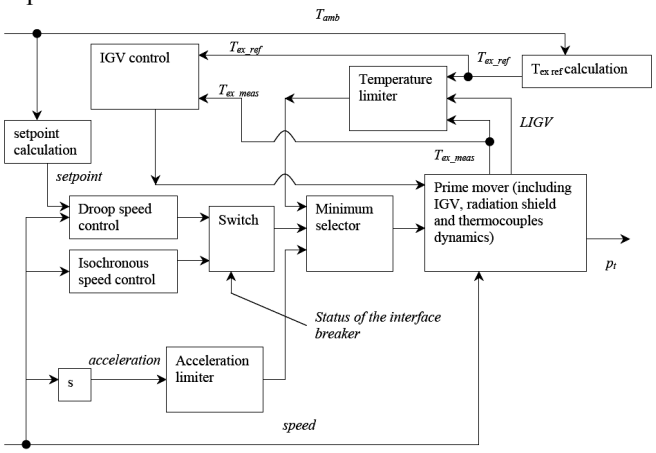

Fig. 2. Overall model of a gas turbine for CHP application

The actual prime mover is essentially a device which can be modelled by a linear model. The control on the prime mover is mainly operated by a speed controller which acts on a fuel request signal: according to the status of connection of the gas turbine to the grid, it can be droop-type (operation with connection to the grid) or isochronous (islanded operation). Another implemented control is the IGV (Inlet Guide Vanes) control which regulates the exhaust temperature by keeping the fuel/air ratio constant (the IGV position in p.u. is called LIGV). Both the speed and the IGV control are "continuous" controls, because they are always in operation.

Besides these two controls, the model includes also two limiters which intervene by reducing the fuel request only when certain variables (rotor acceleration or the temperature of the exhaust gases) overcome user-defined thresholds.

The fuel request is the output of a minimum selector with three inputs: the signals coming from the speed controller, from the acceleration limiter and from the exhaust temperature limiter.

IV. OVERVIEW OF THE GRID UNDER TEST

The test system used for the validation of the fuel cell model consists in a 15 kV distribution grid with one active feeder where both a gas turbine and a fuel cell area located.

Fig. 3 shows the scheme of the grid under test.

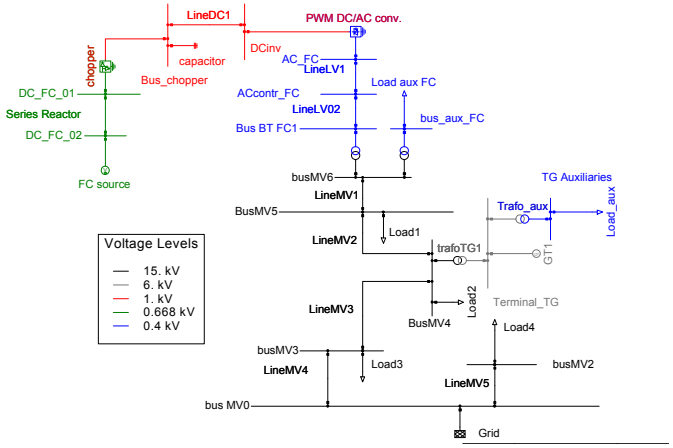

Fig. 3. MV distribution network under study

The two DG sources are endowed with auxiliaries at 400 V. These loads are modelled as dynamic loads with a time constant equal to 0.1 s and with Pf, PV,QV and Qf coefficients suggested in [10]. The fuel cell and the gas turbine ratings are respectively equal to 250 kW and 650 kW. The regulating energy of the equivalent MV grid is 100 MW/Hz.

V. LOAD FOLLOWING INVESTIGATION

As for the load following analysis, the objectives of the study is to assess:

- The distribution system response in case of a setpoint change for the inverter of the fuel cell.
- The reaction of the fuel cell in case of a load ramp of the gas turbine.

TABLE I summarizes the performed simulations on the power system above.

TABLE I
OVERVIEW OF THE SIMULATIONS CARRIED OUT FOR LOAD FOLLOWING ANALYSES

Simulation	Description	Goal
Sim 1	5 kW variation of the setpoint of the fuel cell	To validate the model of the fuel cell
Sim 2	50 kW variation of the setpoint of the fuel cell	To verify the correct operation of the fuel utilization limiter

A. Simulation 1: SOFC active power setpoint variation equal to 5 kW

In this case at t = 20s the setpoint of the active power of the fuel cell undergo an increment (from 150 kW to 155 kW) with a total increase of active power injection equal to 5 kW. Fig. 4 illustrates the fuel cell actual current, the fuel cell current demand and the relevant limits associated with the utilization factor, the voltage at the fuel cell terminal.

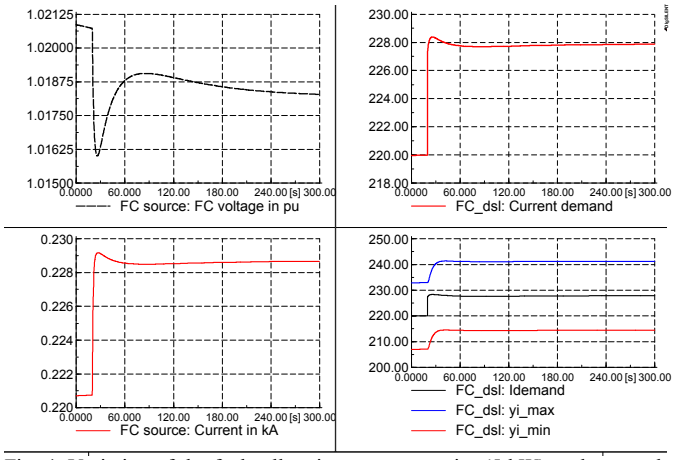

Fig. 4. Variation of the fuel cell active power setpoint (5 kW): voltage at the fuel cell terminal (left top), current demand (right top), actual fuel cell current (left bottom) and current demand with relevant upper and lower limits (right bottom)

It can be noticed that the current demand does not exceed the superior and inferior limits related to the utilization factor.

Fig. 5 shows the partial pressures of hydrogen and oxygen.

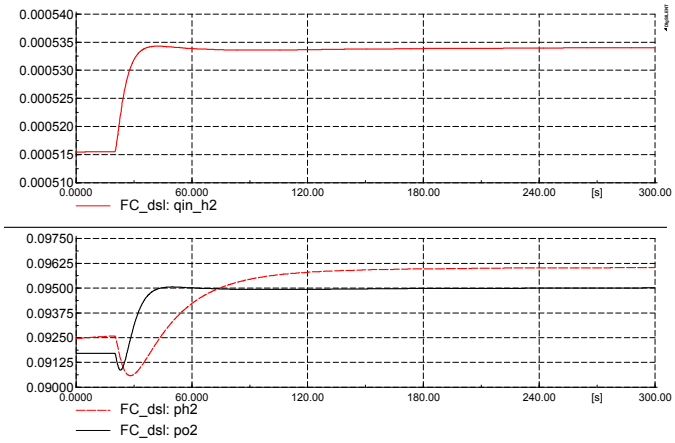

Fig. 5. Variation of the FC setpoint (5 kW): hydrogen input molar flow (top diagram), partial pressures of hydrogen and oxygen (bottom diagram)

In this case the partial pressure of hydrogen initially tends to decrease because the increase of active power setpoint determines an increment of H_2 consumption. After that the increase of the fuel request signal causes an increase of the hydrogen partial pressure. A similar trend can be identified for the oxygen partial pressure.

Fig. 6 illustrates the active power injected by the inverter (top diagram), the duty cycle of the chopper (mid diagram) and the voltage at the DC link. It can be noticed that the chopper control is able to restore the DC voltage at its original value.

At last it is interesting to illustrate the trend of the utilization factor (see Fig. 7). The control implemented in the electromechanical model of the fuel cell allows to restore the optimal value of the utilization factor (0.85).

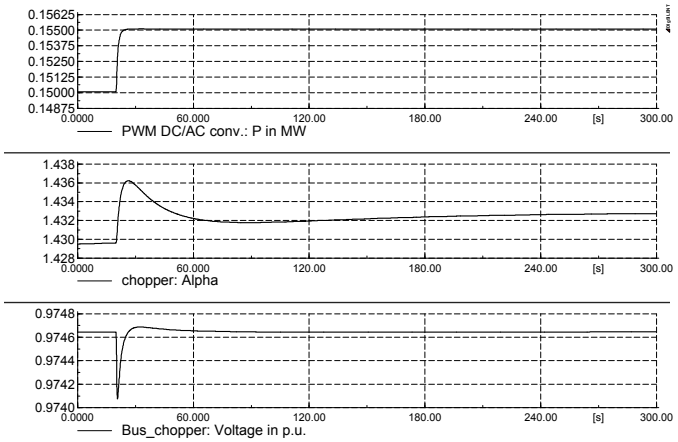

Fig. 6. Variation of the FC setpoint (5 kW): active power injected by the FC inverter (top diagram), duty cycle of the chopper (mid diagram), voltage at the DC link (bottom diagram).

The FC setpoint increase causes an higher consumption of the hydrogen molar flow in the reactions, thus an increase of the utilization factor.

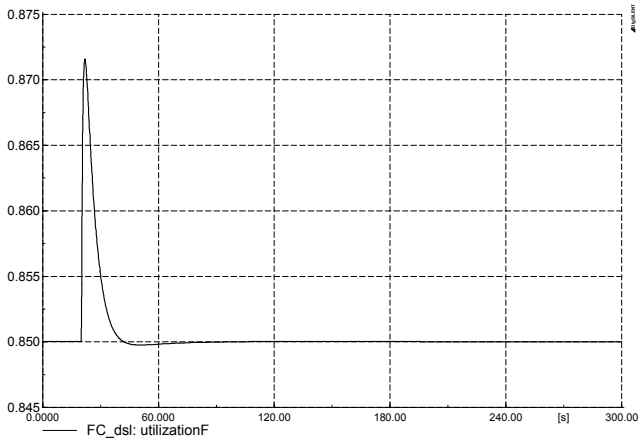

Fig. 7. Variation of the FC setpoint (5 kW): fuel utilization factor

B. Simulation 2: SOFC active power setpoint variation equal to 50 kW

In this case at t=20s the set point of the active power injected by the fuel cell is changed from 150 kW to 200 kW. Fig. 8 shows the fuel cell actual current, the fuel cell current demand and the relevant limits associated with the utilization factor, the voltage at the fuel cell terminal. This case has been analyzed in order to verify the correct operation of the limiter of the fuel utilization factor.

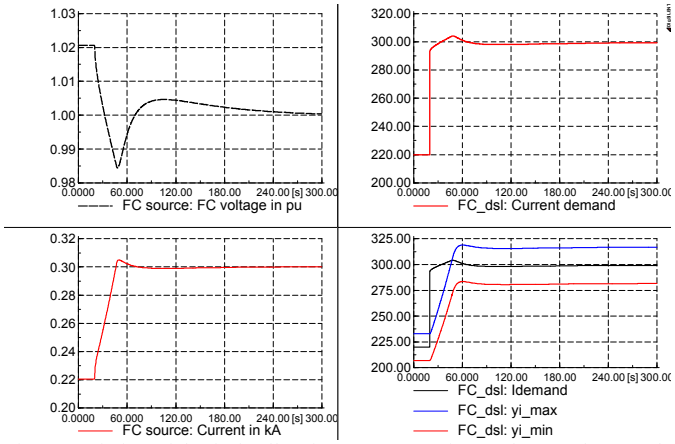

Fig. 8. Variation of the fuel cell active power setpoint (50 kW): voltage at the fuel cell terminal (left top), current demand (right top), actual fuel cell current (left bottom) and current demand with relevant upper and lower limits (right bottom)

In this case the current demand overcomes the upper limit related to the utilization factor (see the black and blue curves in the bottom right diagram of Fig. 8). The current provided by the fuel cell is limited thanks to the intervention of the limiter of the fuel utilization factor. This can be assessed by comparing the actual FC current with the current demand.

Fig. 9 illustrates the utilization factor during this perturbation. It can be noticed the intervention of the limiter which stops the utilization factor increase.

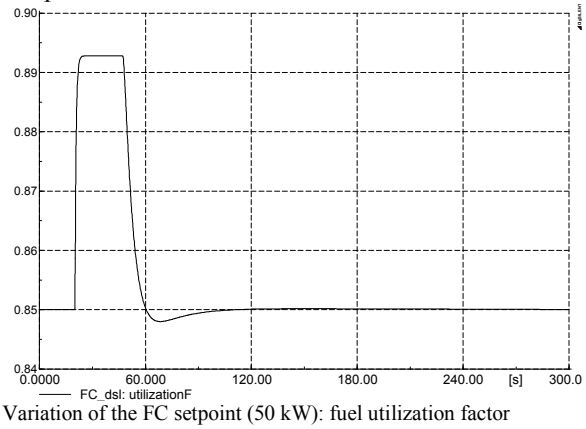

Fig. 9. Variation of the FC setpoint (50 kW): fuel utilization factor

Fig. 10 illustrates the partial pressures of hydrogen and oxygen and the input molar flow of hydrogen.

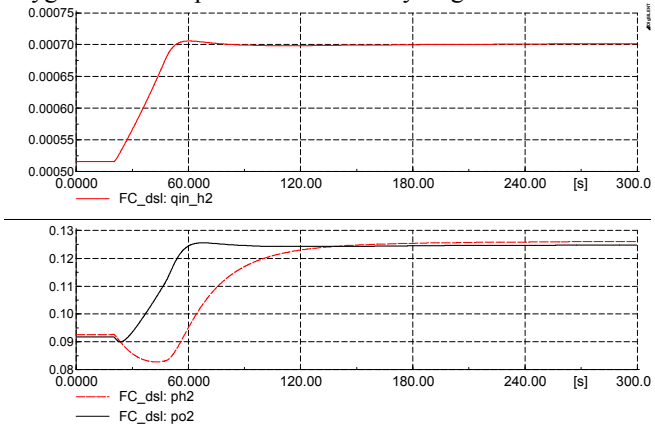

Fig. 10. Variation of the FC setpoint (50 kW): hydrogen input molar flow (top diagram), partial pressures of hydrogen and oxygen (bottom diagram)

Fig. 11 shows the active power injected by the inverter, the control variable of the chopper and the voltage at the DC link.

The current increment causes a decrease of voltage at the DC link. The DC voltage controller intervenes by increasing the duty cycle of the chopper. When the SOFC current becomes stable and decreases, the voltage has a sudden increment and the controller acts by decreasing the duty cycle in order to restore the DC voltage at its initial value.

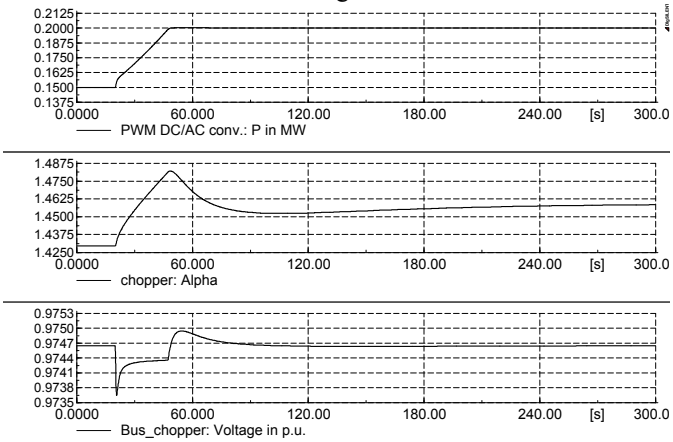

Fig. 11. Variation of the FC setpoint (50 kW): active power injected by the FC inverter (top diagram), duty cycle of the chopper (mid diagram), voltage at the DC link (bottom diagram).

VI. Transient Stability Investigation

This section is devoted to present the response of the power system under study to self-extinguishing three-phase faults. In particular the goal is to evaluate the effect of the disconnection of converter-interfaced DG sources (like the SOFC) on the transient stability of the network.

TABLE II summarizes the simulations which are discussed in the sequel.

TABLE II
SIMULATIONS CARRIED OUT FOR TRANSIENT STABILITY ANALYSIS

Simulation	Description	Goal
Sim 1	150 ms Self-extinguishing three-phase fault applied to bus MV5	To evaluate the behavior of the fuel cell in case of a “close” fault
Sim 2	150 ms Self-extinguishing three-phase fault applied to bus MV2	To evaluate the behavior of the fuel cell in case of a “remote” fault

This study also allows to assess the impact of protections on the transient stability of a distribution grid. In the base case the gas turbine and the fuel cell are respectively injecting 400 kW and 150 kW.

A. Three-phase fault at bus MV5

In this case at t=1s a three-phase self-extinguishing fault is applied to bus MV5. The voltage drop makes the undervoltage protection of the fuel cell intervene. The 150 kW provided by the fuel cell are lost and the distribution network and the gas turbine react. The main contribution is due to the equivalent

MV grid. However the fault causes a transient also in the gas turbine plant. Fig. 12 shows the electric and the mechanical power of the gas turbine, the voltage at its terminal, the speed and the measured (T_{ex_meas}) and the calculated temperature (T_{ex}) of the exhaust gases.

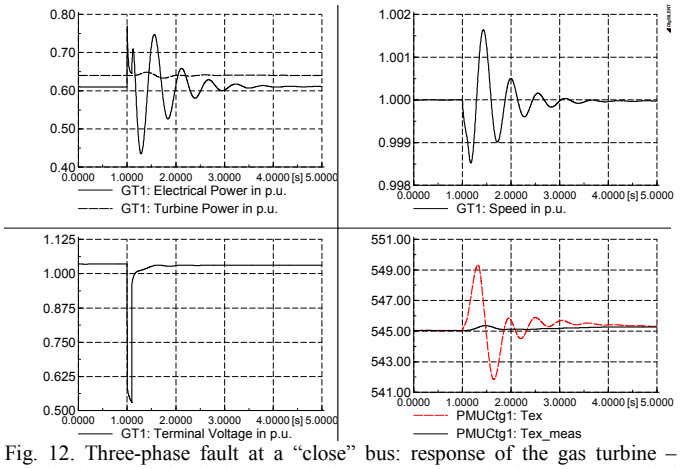

Fig. 12. Three-phase fault at a "close" bus: response of the gas turbine – electrical and mechanical power (left top), rotor speed (right top), terminal voltage (left bottom), measured and calculated temperature of the exhaust gases (right bottom)

A little increment of the mechanical power can be recognized due to the droop response of the machine. Also the temperature of the exhaust gases undergoes a little increase (equal to about 0.4°C).

Fig. 13 indicates the speed-angle plane for the gas turbine. It clearly shows that the final angle is different from the initial one due to the loss of injected power because of the fuel cell disconnection.

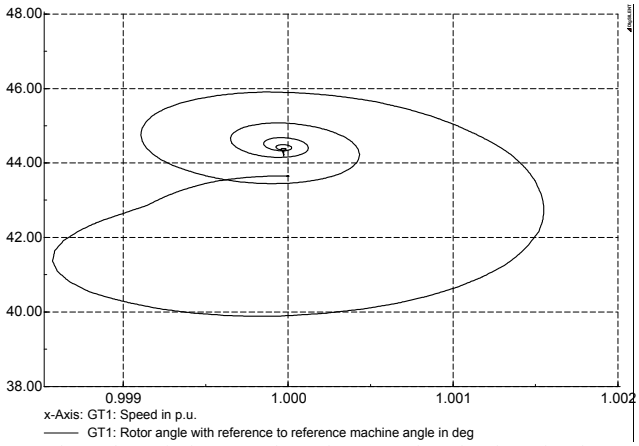

Fig. 13. Three-phase fault at a "close" bus: speed-angle plane for the gas turbine

B. *Three-phase fault at bus MV2*

The same auto-extinguishing fault is applied to a "remote" bus (MV2) at t=1s. The fault does not cause the FC to be disconnected. Fig. 14 shows the transient of the gas turbine.

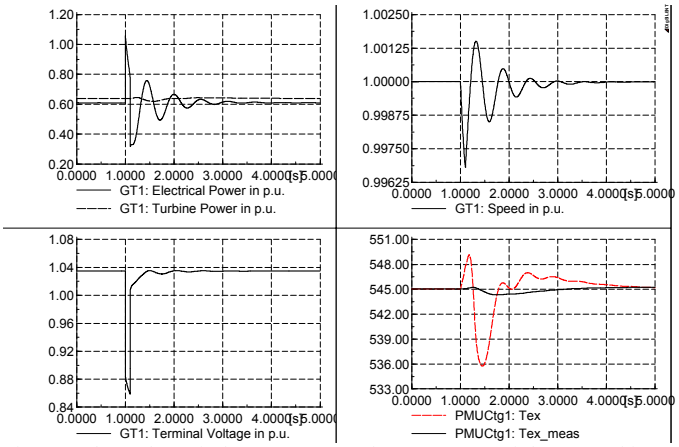

Fig. 14. Three-phase fault at a "remote" bus: response of the gas turbine – electrical and mechanical power (left top), rotor speed (right top), terminal voltage (left bottom), measured and calculated temperature of the exhaust gases (right bottom)

Fig. 15 shows the speed-angle plane of the gas turbine.

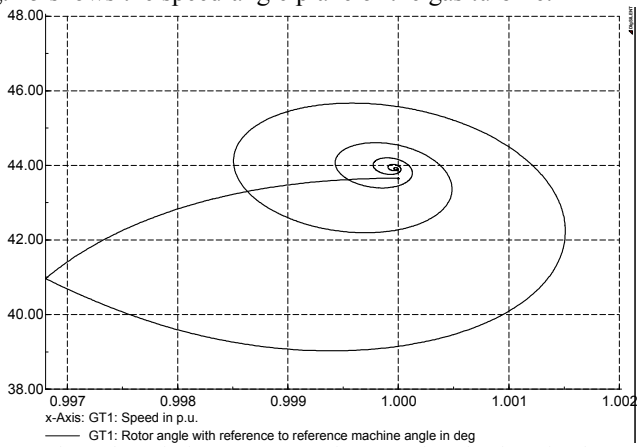

Fig. 15. Three-phase fault at a "remote" bus: speed-angle plane for the gas turbine

It can be noticed that the final angle coincides with the initial angle. In fact in this case after the auto-extinguishing fault the system comes back to the initial operating condition: the fault does not make the undervoltage protection of the SOFC intervene.

VII. Conclusions

The paper presents a dynamic model of a Solid Oxide Fuel Cell which can be used both for load following and for stability analyses. The model has been validated on a MV distribution network where also a gas turbine has been inserted. After the thorough presentation of the subsystems composing the overall SOFC model (and of its relevant protections), a brief description of the gas turbine model is performed. The load following analysis allows to assess the correct operation of the limiter of the fuel utilization factor and of the controls related to the power electronic converters. The transient stability analysis is aimed at evaluating the response of the network in case of auto-extinguishing faults in the test system in presence of a converter-interfaced DG source like the SOFC.

REFERENCES

[1] R. Lasseter, "Control of Distributed Resources", IREP 1998, Bulk Power System Dynamics and Control IV - Restructuring, August 24-28, Santorini, Greece

[2] Fuel cell handbook, 7th edition, 2004

[3] J. Padulles, G. W. Ault, J. R. McDonald, "An integrated SOFC plant dynamic model for power systems simulation", Journal of Power Sources, Elsevier, 2000, pp. 495-500

[4] Y. Zhu, K. Tomsovic, "Development of models for analyzing the load following performance of microturbines and fuel cells", Electric Power Systems Research, Elsevier, 2002, pp.1-11

[5] DigSILENT PowerFactory, User's Manual, version 13.2

[6] D. Georgakis, S. Papathanassiou, S. Mania, "Modeling and control of a small scale grid-connected PEM fuel cell system", Proc. PESC'05, June 2004, Recife, Brazil

[7] M. Nagpal, A. Moshref, G. K. Morison and P. Kundur, "Experience with Testing and Modeling of Gas Turbines", presented at IEEE Winter Meeting panel session Experience with Modeling of Gas turbine and Combined Cycle Power Plants, sponsored by the Power System Dynamic Performance Committee, Jan 2001, Columbus OH

[8] W. I. Rowen, "Simplified Mathematical representation of single shaft gas turbines in mechanical drive service", Turbomachinery International, July/August 1992, pp. 26-32

[9] A. Bagnasco, B. Delfino, G. B. Denegri, and S. Massucco, "Management and dynamic performances of combined cycle power plants during parallel and islanding operation," *IEEE Trans. Energy Conversion*, vol. 13, pp. 194–201, June 1998.

[10] P. Kundur, *Power System Stability and Control*, MacGraw-Hill, New York, 1994